

X-ray-induced disordering of the dimerization pattern and apparent low-temperature enhancement of lattice symmetry in spinel CuIr_2S_4

H. Ishibashi^{1,2}, T. Y. Koo¹, Y. S. Hor¹, A. Borissov¹, Y. Horibe^{3,4}, P. G. Radaelli^{5,6}, S-W. Cheong^{1,3}, and V. Kiryukhin¹

(1) *Department of Physics and Astronomy, Rutgers University, Piscataway, New Jersey 08854*

(2) *Department of Materials Science, Osaka Prefecture University, Sakai, Osaka 599-8531, Japan*

(3) *Bell Laboratories, Lucent Technologies, Murray Hill, New Jersey 07974*

(4) *Department of Materials Science and Engineering and Kagami Memorial Laboratory for Materials Science and Technology, Waseda University, Shinjuku-ku, Tokyo 169, Japan*

(5) *ISIS Facility, Rutherford Appleton Laboratory, Chilton, Didcot, Oxfordshire, OX11 0QX, United Kingdom*

(6) *Dept. of Physics and Astronomy, University College London, Gower St., London, WC1E 6BT, United Kingdom*

(October 25, 2018)

At low temperatures, spinel CuIr_2S_4 is a charge-ordered spin-dimerized insulator with triclinic lattice symmetry. We find that x-rays induce a structural transition in which the local triclinic structure is preserved, but the average lattice symmetry becomes tetragonal. These structural changes are accompanied by a thousandfold reduction in the electrical resistivity. The transition is persistent, but the original state can be restored by thermal annealing. We argue that x-ray irradiation disorders the lattice dimerization pattern, producing a state in which the orientation of the dimers is preserved, but the translational long-range order is destroyed.

PACS numbers: 75.50.-y, 61.10.Nz, 72.80.Ga, 61.80.Cb

Spinel compounds AB_2X_4 (X is O, S, Se, or Cl) have attracted much attention over the last decade because they exhibit a large variety of interesting ground states, including superconductivity, cooperative antiferromagnetism, heavy fermion, and charge-ordered and spin-dimerized states [1,2]. The panoply of different properties exhibited by spinels results from the interplay of Coulomb interactions, effects of frustrated magnetism, and electron-lattice interaction. The corner sharing tetrahedral network of B sites in the spinel structure can accommodate a large number of different charge ordering patterns. In fact, some of the most complex charge-ordering patterns reported to date are found in spinel compounds [3,4]. The same tetrahedral network gives rise to geometric magnetic frustration when the ions occupying the B site are magnetic. The electronic and magnetic states realized in such a complex environment are often multi-degenerate and strongly fluctuating. Because of these complexity, a number of properties of the spinels remain poorly understood. Spinel, therefore, are important subjects of research in the physics of strongly correlated materials. In addition, some of these compounds, such as the lithium manganese spinels used in battery cathodes and the ferrites used in microwave applications, are of substantial technological importance.

Chalcogenide spinel CuIr_2S_4 has attracted attention because this compound undergoes a sharp metal-insulator transition at $T_{MI} \approx 230$ K [5]. The low-temperature insulating state is nonmagnetic. NMR and photoemission experiments have shown that the Cu ion is monovalent in the insulating phase, and therefore the nominal valence of the iridium atoms is 3.5 [6]. It was

proposed that charge ordering of Ir^{3+} ($S=0$) and Ir^{4+} ($S=1/2$) ions is the origin of the metal-insulator transition in CuIr_2S_4 [5], and that some kind of spin dimerization is responsible for the nonmagnetic nature of the insulating phase.

Recent experimental determination of the low-temperature structure [3] has provided very strong evidence that this scenario is correct. Specifically, these experiments have shown that the Ir sublattice consists of two types of Ir bi-capped hexagonal rings, which were described as Ir_8^{3+} and Ir_8^{4+} octamers. The $S=1/2$ Ir^{4+} ions were found to form structural dimers, which were also identified as spin dimers. The magnitude of the lattice distortion due to this dimerization is truly remarkable: the Ir-Ir distance in the dimers is $\sim 3.0\text{\AA}$, while all the other Ir-Ir nearest neighbor distances are between 3.43 and 3.66 \AA . Inset in Fig. 1 illustrates the low-temperature charge ordering and spin-dimerization pattern reported in [3]. The low-temperature state possesses triclinic symmetry [7,3]. However, for simplicity, we describe the structure of CuIr_2S_4 using the conventional cubic spinel unit cell, which is not the true unit cell at low temperatures.

In this work, we report high-resolution x-ray powder diffraction and simultaneous electrical resistance measurements on CuIr_2S_4 . We find that at low temperatures, x-rays induce a triclinic-to-tetragonal structural transition in which the electrical resistivity is reduced by a factor of 10^3 . The transition is persistent, but the original state can be restored by heating above $T \sim 100$ K and subsequent cooling. To our knowledge, the only other example of such a dramatic reversible x-ray-induced struc-

tural change is found in perovskite manganites, in which x-rays convert a charge ordered insulator to ferromagnetic metal [8]. In our samples, all the Bragg peaks in the x-ray converted state can be accounted for using the tetragonal $I4_1/amd$ space group. However, analysis of the diffuse x-ray scattering in the tetragonal state shows that the triclinic structure is preserved locally. Therefore, x-ray irradiation changes only the average (or global) symmetry. We argue that this apparent change in the lattice symmetry is caused by x-ray-induced disordering of the lattice dimerization pattern, in which the orientation of the Ir^{4+} dimers is preserved. Tetragonal CuIr_2S_4 provides, therefore, an interesting example of a state possessing rotational, but not translational, long range dimer order.

Polycrystalline samples of CuIr_2S_4 were prepared by a solid reaction method. The mixtures of Cu, Ir, and S powders were heated in an evacuated quartz tube at 800-900 °C for 8 days. The samples were then ground, pressed into a pellet, and sintered in vacuum at 900 °C for another 3 days. X-ray powder diffraction measurements were carried out at beamlines X20C and X25 at the National Synchrotron Light Source. An x-ray beam was focused by a mirror, monochromatized by a double-crystal Si (111) monochromator, and analyzed with Ge (111) crystal. The wavelengths used were $\lambda=1.513$ and 1.5406 Å, the beam size was ~ 1 mm², and the typical intensity was $3 \cdot 10^{11}$ photons/sec. The sample was mounted in a closed-cycle refrigerator ($T=6$ -300 K). The powder patterns were measured using the $\theta/2\theta$ step scanning mode. For electrical resistivity measurements, four gold contacts were evaporated on the surface of the polycrystalline sample. The x-ray beam was hitting the sample in between the contacts, and x-ray diffraction and electrical resistance measurements were done simultaneously. Neutron powder diffraction data were collected using the HRPD high-resolution powder diffractometer at the ISIS facility.

Fig. 1 shows partial x-ray scans taken at $T=6$ K and $T=200$ K. Note that the x-ray intensity is shown on a logarithmic scale. The $T=6$ K scan was taken after several hours of initial exposure to x-rays. All the Bragg peaks at $T=6$ K can be indexed assuming the tetragonal symmetry with the space group $I4_1/amd$ and lattice constants $a=6.8766$ Å and $c=10.039$ Å, with the a and b axes pointing along the (110) and (1-10) directions in the cubic spinel unit cell. At $T=200$ K, the structure is triclinic. For $T>T_{MI} \approx 230$ K, CuIr_2S_4 exhibits an undistorted cubic spinel structure. In this work, all the Bragg peaks are indexed using the cubic spinel unit cell with lattice constant $a \sim 9.8$ Å. Note, this indexing scheme is only approximate for $T < T_{MI}$. In the triclinic state, a number of peaks that are not present in the cubic and the tetragonal phase appear (see Fig. 1). We refer to these peaks as superlattice peaks.

According to our neutron diffraction measurements

taken after the sample was equilibrated for 12 h at $T=4$ K, the low-temperature state of CuIr_2S_4 is triclinic. The tetragonal state is induced by x-rays. Figure 2(a) shows that a 30 min x-ray exposure completely destroys the superlattice peaks. At the same time, the resistance of the sample is significantly reduced, see Fig 2(b). When the x-rays are switched off, the resistance increases abruptly (most likely due to beam heating effects), and then keeps increasing with a time constant $\tau > 5$ h. It is possible, therefore, that the x-ray induced state is metastable. Even after a 10 h wait, however, the resistance does not reach a third of its original value, and no detectable superlattice peaks are observed after 24 h. In our experimental geometry, x-rays penetrated only ~ 2 μm into the sample, and therefore only a small surface layer of the sample was undergoing the x-ray-induced transition. Assuming that the thickness of this layer equals to the x-ray penetration depth, we estimate that the resistivity of the tetragonal state is approximately 2 Ωcm. This is at least 3 orders of magnitude smaller than the resistivity of the triclinic phase in polycrystalline CuIr_2S_4 [5,9].

The triclinic state recovers when the sample is heated above 100 K, even in the presence of x-rays. In Figure 3, scans in the vicinity of the (4,0,0) main Bragg peak and the (1.5,1.5,1.5) superlattice peak taken on heating at different temperatures are shown. The triclinic state manifests itself by splitting of the tetragonal peaks and by the appearance of the superlattice peaks. The superlattice peaks are very broad at low temperatures. A careful examination of the x-ray scan at $T=6$ K in Fig. 1 shows that enhanced diffuse scattering exhibiting broad features with maximums near the superlattice peak positions is present in the tetragonal state. Such a broad feature can be seen, for example, at the (0,1,1) superlattice peak position at $2\theta=12.7^\circ$. Broadening of the diffraction peaks is associated with finite correlation length of the ordered state. Therefore, short-range-ordered triclinic regions, and the associated Ir^{4+} dimers, are present even in the x-ray converted state. Unlike the superlattice peaks, the main Bragg peaks remain narrow in the entire temperature range.

Figure 4 shows the integrated intensity of the (0,1,1) and (1.5,1.5,1.5) superlattice peaks, and the superlattice peak width taken at different temperatures on heating from the x-ray converted state. These data were obtained from the scans shown in Figs. 1, 3 using Lorentzian fits. The integrated intensity is the same in both the triclinic and the tetragonal states, within experimental errors. Therefore, on the local level, the structure is triclinic everywhere in the x-ray converted state. The correlation length of the triclinic lattice distortion, estimated from the width of the (0,1,1) peak, is $\xi_{tr} \sim 30$ Å at $T=6$ K.

Dimerization of Ir^{4+} is the dominant source of the triclinic lattice distortion, and therefore the long-range correlation between the dimers is lost in the tetragonal state. We propose the following scenario of the x-ray induced

transition. X-rays remove localized electrons from the Ir atoms, thereby instantaneously destroying local charge-ordering and lattice dimerization pattern. The electrons quickly relax, and the charge-ordering is restored. However, Ir^{4+} dimers do not necessarily form in the original places. This is, in fact, not unexpected, if one takes into account that slowly propagating elastic interactions play a dominant role in the formation of the dimerization pattern in CuIr_2S_4 . The Coulomb interaction is less important in this compound, as indicated by the breakdown of the Anderson's condition which requires that two Ir^{3+} and two Ir^{4+} ions are present in every Ir tetrahedron (see inset in Fig. 1). It is interesting to note that the correlation length ξ_{tr} is large enough to accommodate several Ir octamers. This indicates that the Ir^{4+} dimers still tend to form the octamer units in the tetragonal state, and therefore these octamers are quite robust.

Rietveld refinement of the powder data in the x-ray converted tetragonal state can only provide the average structure. In fact, in the $I4_1/amd$ group, all the Ir atoms are equivalent, and no direct information about the Ir charge order can be obtained in a conventional refinement. Experiments on single crystals will eventually be required to determine the local structure of the tetragonal state, and XPS or NEXAFS measurements will be needed to study the valence state of the Ir atoms in the irradiated samples. We have, however, attempted the Rietveld refinement of the powder data at $T=6$ K putting Ir^{3+} ions in the $8d$ site with occupation 0.5, and Ir^{4+} ions in the $16h$ site with occupation 0.25. The refinement produced two Ir^{4+} ions in each $16h$ site displaced along the $[110]$ cubic direction with respect to each other. Since in the triclinic state the Ir^{4+} dimers form along the same direction [10], this result is consistent with the assumption that uncorrelated dimers are present in the sample. It also indicates that the dimers in the x-ray converted state form along the same direction as in the triclinic phase. Moreover, the intradimer distance obtained in our refinement, 3.09 Å, is close to the actual value found in the triclinic state. While the overall quality of the fit is only average ($R_{wp}=0.100$), the fit is consistent with the disordering scenario proposed above. Further details of the Rietveld refinement will be given elsewhere [9].

In addition to the results of the Rietveld refinement, the increased value of the c lattice constant in the tetragonal state provides an evidence that the Ir^{4+} dimers remain contained in the ab plane and, therefore, do not change their orientation. The long-range translational order of the dimers, on the other hand, is clearly destroyed in the tetragonal state. An interesting question, which requires further investigation, is whether the tetragonal state in CuIr_2S_4 could be considered a thermodynamic phase, with some properties, possibly, resembling those of liquid crystal phases. To answer this question, the equilibrium thermal properties of the tetragonal state need to be investigated. As was mentioned above, the x-ray

induced state is in all likelihood metastable. However, it might be possible that the equilibrium tetragonal state can be induced by other sources of disorder. In particular, static disorder from chemical substitution appears to be promising. To test this proposal, experiments with $\text{Cu}(\text{Ir,Cr})_2\text{S}_4$ samples are currently under way.

The reduced electrical resistivity in the x-ray converted state most likely results from the imperfections in the charge order. Charge-disordered conducting regions might form, for instance, at the boundaries between the ordered triclinic domains. Consistent with this assumption, the resistivity characteristic to the triclinic state is recovered on heating, as these imperfections disappear and the long-range ordered triclinic state is restored, see Fig. 4(c).

Finally, we note that in a recent paper, Sun *et al.* reported an electron diffraction experiment suggesting a structural transition in CuIr_2S_4 at $T < \sim 50$ K [11]. We speculate that this transition is of the same nature as the x-ray induced transition described above, and that it is induced by an electron beam.

In summary, we find that x-rays induce an apparent triclinic-to-tetragonal transition in CuIr_2S_4 at low temperatures. In addition to the drastic structural changes, x-ray irradiation reduces the electrical resistivity by at least 3 orders of magnitude. The triclinic state can be recovered by thermal annealing. We argue that the transition results from the x-ray-induced disorder in the Ir^{4+} dimerization pattern, in which the orientation of the dimers is preserved, but the translational long-range order is destroyed.

We are grateful to L. Berman, C. H. Chen, J. P. Hill, and A. J. Millis for important discussions. This work was supported by the NSF under grants No. DMR-0103858, and DMR-0093143, and by A. P. Sloan Foundation (VK).

-
- [1] A. P. Ramirez, *Ann. Rev. Mater. Sci.* **24**, 453 (1994); J. F. Greedan, *J. Mater. Chem.* **11**, 37 (2001).
 - [2] A. P. Ramirez, R. J. Cava, J. Krajewski, *Nature (London)* **386**, 156 (1997); N. Matsumoto, R. Endo, S. Nagata, T. Furubayashi, T. Matsumoto, *Phys. Rev. B* **60**, 5258 (1999), and references therein.
 - [3] P. G. Radaelli, Y. Horibe, M. J. Gutmann, H. Ishibashi, C. H. Chen, R. M. Ibberson, Y. Koyama, Y-S. Hor, V. Kiryukhin, and S-W. Cheong, *Nature (London)* **416**, 155 (2002).
 - [4] J. Rodriguez-Carvajal, G. Rouse, C. Masquelier, and M. Hervieu, *Phys. Rev. Lett.* **81**, 4660 (1998).
 - [5] T. Furubayashi, T. Matsumoto, T. Hagino, and S. Nagata, *J. Phys. Soc. Jpn.* **63**, 3333 (1994).
 - [6] K. Kumagai, S. Tsuji, T. Hagino, and S. Nagata, in *Spectroscopy of Mott Insulators and Correlated Metals*, edited

by A. Fujimori and Y. Tokura (Springer, Berlin, 1995); J. Matsuno, T. Mizokawa, A. Fujimori, D. A. Zatsepin, V. R. Galakhov, E. Z. Kurmaev, Y. Kato, and S. Nagata, Phys. Rev. B **55**, R15979 (1997).

- [7] H. Ishibashi, T. Sakai, and K. Nakahigashi, J. Magn. Magn. Mater. **226-229**, 233 (2001).
- [8] V. Kiryukhin, D. Casa, J. P. Hill, B. Keimer, A. Vigliante, Y. Tomioka, and Y. Tokura, Nature (London) **386**, 813 (1997).
- [9] H. Ishibashi, unpublished.
- [10] And the symmetry-related [1,-1,0] direction. All the Ir⁴⁺ dimers are contained in one plane.
- [11] W. Sun, T. Kimoto, T. Furubayashi, T. Matsumoto, S. Ikeda, and S. Nagata, J. Phys. Soc. of Japan **70**, 2817 (2001).

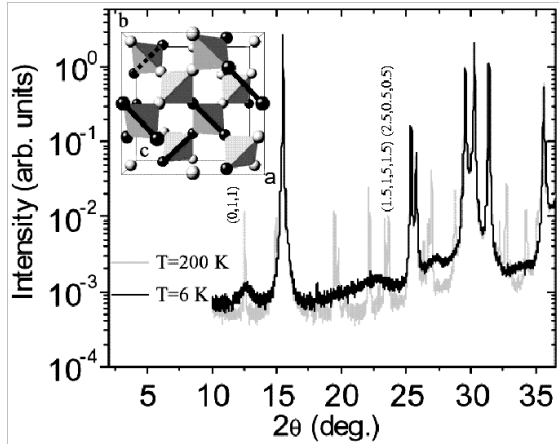


FIG. 1. X-ray powder scans at T=200 K and T=6K, $\lambda=1.5406\text{\AA}$. The inset shows the charge ordering pattern in the triclinic state. Ir³⁺ and Ir⁴⁺ ions are shown in white and black, respectively. Black bonds indicate dimerized Ir⁴⁺ ions.

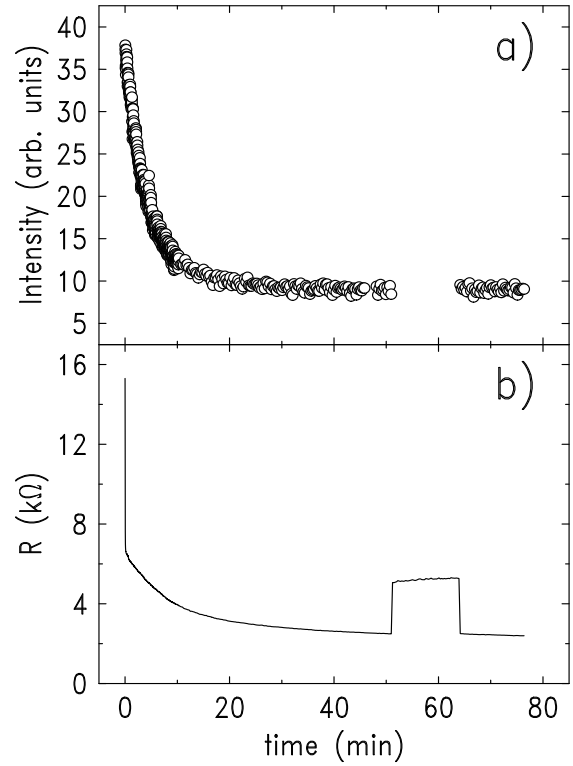


FIG. 2. X-ray exposure dependence of (a) the intensity of the (2,2,1) superlattice peak and (b) electrical resistance at T=10 K. X-rays were switched off between $t=51$ min and $t=64$ min.

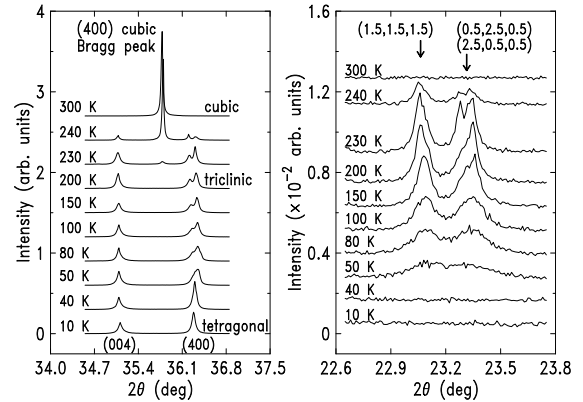


FIG. 3. X-ray scans in the vicinity of the (400) cubic Bragg peak, and the (1.5,1.5,1.5), (0.5,2.5,0.5), and (2.5,0.5,0.5) superlattice peaks at various temperatures, taken on heating. X-ray wavelength $\lambda=1.513\text{\AA}$.

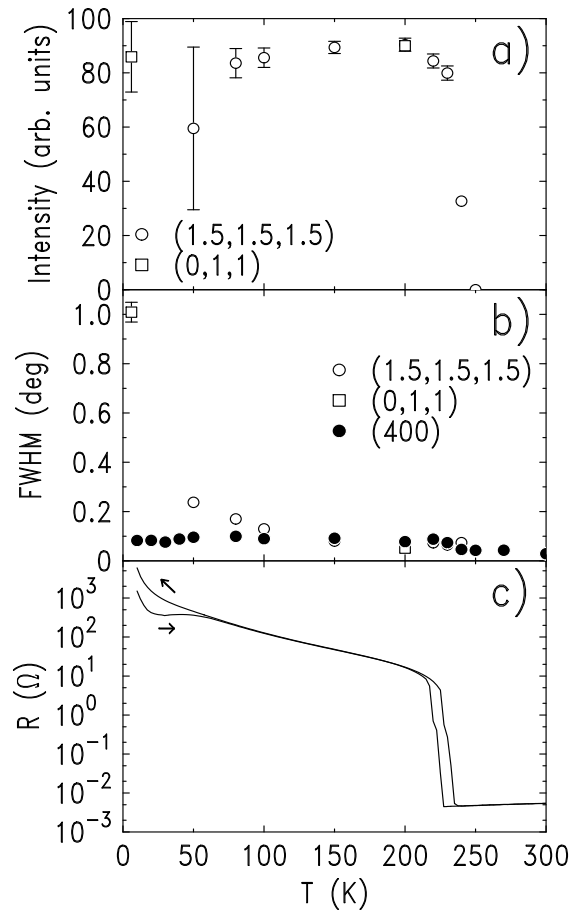


FIG. 4. Temperature dependence of (a) the integrated intensity of the $(1.5, 1.5, 1.5)$ and $(0, 1, 1)$ superlattice peaks, (b) full width at half maximum of the same superlattice peaks and of the (400) Bragg peak, and (c) electrical resistance. The data were taken on heating from the x-ray converted state. Electrical resistance taken on cooling with no x-rays present is also shown. The $(0, 1, 1)$ peak intensity in (a) was normalized to match the $(1.5, 1.5, 1.5)$ intensity at $T=200$ K.